01 Jan 1993

Defect Structure Of Y1-ycaymno3 And La1-ycaymno3. I. Electrical Properties

J. W. Stevenson

M. M. Nasrallah

Harlan U. Anderson
Missouri University of Science and Technology, harlanua@mst.edu

Don M. Sparlin
Missouri University of Science and Technology, sparlin@mst.edu

Recommended Citation

J. W. Stevenson et al., "Defect Structure Of Y1-ycaymno3 And La1-ycaymno3. I. Electrical Properties," *Journal of Solid State Chemistry*, vol. 102, no. 1, pp. 175 - 184, Elsevier, Jan 1993.
The definitive version is available at https://doi.org/10.1006/jssc.1993.1020

JOURNAL OF SOLID STATE CHEMISTRY 102, 175–184 (1993)

Defect Structure of $Y_{1-y}Ca_yMnO_3$ and $La_{1-y}Ca_yMnO_3$

I. Electrical Properties

J. W. STEVENSON, M. M. NASRALLAH, H. U. ANDERSON, AND D. M. SPARLIN*

*Ceramic Engineering Department and *Physics Department, University of Missouri–Rolla, Rolla, Missouri 65401*

Received February 14, 1992; in revised form June 8, 1992; accepted June 24, 1992

Electrical conductivity and the Seebeck coefficient of compositions in the system $Y_{1-y}Ca_yMnO_3$ and $La_{1-y}Ca_yMnO_3$ were studied to determine the mechanism of electrical transport and defect structure. Electrical conduction appeared to occur via a small polaron hopping mechanism for compositions with $0.30 \leq y \leq 0.80$. The Seebeck coefficient data did not support the assumption that Mn is present in Ca-doped Mn perovskites only in the +3 and +4 valence states. A new defect model was developed which includes the thermally excited disproportionation of Mn^{3+} into Mn^{2+} and Mn^{4+} pairs. The Seebeck data were explained with this model by assuming that divalent Mn cations were site blockers in the conduction process. © 1993 Academic Press, Inc.

1. Introduction

Perovskite-type oxides are used as high-temperature electrode materials due to their high electrical conductivity and stability in oxidizing atmospheres at elevated temperatures. The current cathode material for solid oxide fuel cell (SOFC) applications is Ca- or Sr-doped $LaMnO_3$. $La_{0.8}Sr_{0.2}MnO_3$ exhibits adequate electrical conductivity for the cathode application (*1*), but its thermal expansion is higher than that of the yttria-stabilized zirconia electrolyte (*2*) and it has limited stability in reducing atmospheres (*3*). Stability in a reducing environment is desirable given the likelihood of crack formation during operation of the cell.

Since acceptor-doped $LaMnO_3$ is not an ideal cathode material, other perovskite oxides should be considered for this application. $LaCrO_3$ and $YCrO_3$ materials have much lower electrical conductivity (*4–6*). $LaCoO_3$ compounds can exhibit good conductivity, but their thermal expansions are too high and chemical reaction with the electrolyte can rapidly degrade cathode performance (*7, 8*). Given the relative success of $LaMnO_3$ based materials as SOFC cathodes, it seemed appropriate to consider the related system $Y_{1-y}Ca_yMnO_3$. Accordingly, a thorough study of the electrical and thermogravimetric behavior of compositions in this system was performed. Since it is important to understand the mechanism of electrical conduction (and therefore the defect structure) of electrode materials, the experimental data were analyzed with respect to a new defect model which incorporates the thermally excited disproportionation of Mn^{3+} into Mn^{2+} and Mn^{4+} pairs. Compositions in the $La_{1-y}Ca_yMnO_3$ system were also studied in order to extend the model to low Ca contents. In this paper, the model is applied to the behavior of the

0022-4596/93 $5.00

compositions in air. The behavior in reduced atmospheres will be discussed in Part II.

2. Experimental Procedure

Compositions within the $Y_{1-y}Ca_yMnO_3$ system, y ranging from 0.00 to 1.00 in increments of 0.10, were synthesized from yttrium nitrate, calcium carbonate, and manganese nitrate solution via a polymeric precursor technique (*9*). Calcination at 1125 K for 8 hr was followed by sintering in air for 2 hr. Sintering temperatures were 1623 K for $0.00 \leq y \leq 0.40$, 1573 K for $0.50 \leq y \leq 0.60$, 1523 K for $0.70 \leq y \leq 0.90$, and 1373 K for $y = 1.00$. Compositions in the system $La_{1-y}Ca_yMnO_3$ ($y = 0.00, 0.20, 0.40$, and 0.60) were also synthesized (using lanthanum carbonate as the La^{3+} source). These specimens were sintered in air for 2 hr at 1623 K.

The ac conductivity was measured with a 4-point, 4-wire technique using a Stanford Research Systems SR510 lock-in amplifier with a Hewlett–Packard Model 200 CD oscillator. Frequencies of 100 and 1000 Hz were used. The applied voltage was approximately 0.5 V. Specimen resistances were on the order of 0.1 to 1 ohm.

Seebeck coefficients were measured using alumina holders equipped with Pt wire coil heaters to provide the necessary temperature gradients. The temperature at each end of the specimen was measured with Type S thermocouples while the Seebeck voltage was measured using the Pt leg of each thermocouple and a Keithley 197 Autoranging DMM. The Seebeck coeffcient was determined by applying a temperature gradient of approximately 25 K along the length of the specimen and repeatedly measuring the temperature difference and the corresponding Seebeck voltage. In this manner 20 points were taken, with the slope of the resulting line determined by least-square analysis to give the Seebeck coefficient. This experimental Seebeck voltage was corrected for the thermopower of Pt to yield the Seebeck coefficient of the specimen.

3. Results and Discussion

X-ray diffraction was performed on the synthesized powders to determine the phases present. $YMnO_3$ has two polymorphs. Under some conditions (primarily at high pressure and high temperature) it is an orthorhombic perovskite (*10*), but generally it crystallizes in a hexagonal nonperovskite structure (*11*). The lack of stability of the perovskite form of $YMnO_3$ can be attributed to the fact that Y^{3+} (with an ionic radius of 1.18 Å (*12*)) is nearly too small to act as the *A* cation in the structure (compare with La^{3+}, with an ionic radius of 1.36 Å) when Mn is the *B* cation. The hexagonal structure allows the Y^{3+} to have a smaller coordination number more suitable to its size. After calcination at 1123 K, the $YMnO_3$ end member appeared to exist in both the hexagonal nonperovskite and orthorhombic perovskite phases. X-ray diffraction of powder which had been recalcined at 1473 K revealed only the hexagonal phase. The $CaMnO_3$ end member was a cubic perovskite. For intermediate compositions of $Y_{1-y}Ca_yMnO_3$ with y between 0.30 and 1.00, a single-phase orthorhombic perovskite solid solution was obtained. The degree of orthorhombic distortion decreased with increasing Ca^{2+} content. Compositions with $y = 0.10$ or 0.20 contained two phases; these results are consistent with a previous study (*13*) in which a miscibility gap was found to exist in this system for $\approx 0.05 \leq y \leq 0.25$. Due to the two-phase nature of $Y_{0.9}Ca_{0.1}MnO_3$ and $Y_{0.8}Ca_{0.2}MnO_3$, it was decided that only compositions with $y \geq 0.30$ merited further attention. The calculated relative densities (saturated-suspended weight method) were approx. 85% for $CaMnO_3$

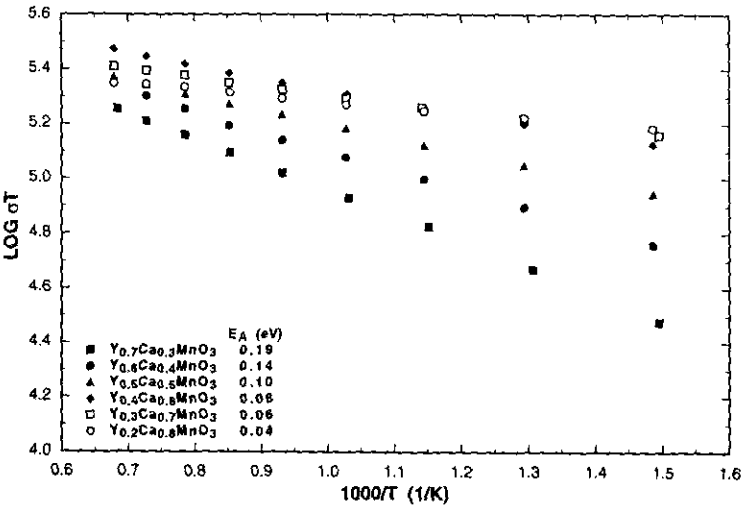

FIG. 1. Log σT vs $1000/T$ in air for the indicated compositions. σ is in units of S/cm. Activation energies are listed in units of eV.

and 90 to 93% for the intermediate compositions.

The ac electrical conductivity of $Y_{1-y}Ca_yMnO_3$ ($0.30 \leq y \leq 1.00$) was measured in air as a function of temperature. Previous investigations (*14–16*) have indicated that manganite perovskites conduct by a small polaron mechanism, so that charge migration through the crystal occurs by a thermally-activated hopping mechanism. For small polaron conductors, a plot of log σT (for the adiabatic case) or log $\sigma T^{3/2}$ (for the nonadiabatic case) vs reciprocal absolute temperature should produce a straight line, with the slope representing $(-E_A/2.303k)$, where E_A is the activation energy and k is Boltzmann's constant. In $Y_{1-y}Ca_yMnO_3$, slightly higher linearity was obtained for the adiabatic assumption. Figure 1 shows log σT vs $1000/T$ for $0.30 \leq y \leq 0.80$. The high linearity for $0.30 \leq y < 0.80$ is consistent with small polaron conduction. For $y \geq 0.80$, the linearity decreased abruptly with increasing Ca content, suggesting that a simple small polaron mechanism does not apply for these compositons. The calculated activation energies are given in the legend of Fig. 1. Kuo *et al.* (*1*) reported activation energies for compositions in the system $La_{1-y}Sr_yMnO_3$ to be 0.19, 0.16, and 0.09 eV for $y = 0.05$, 0.10, and 0.20, respectively. Karim and Aldred (*4*) obtained activation energies between 0.192 and 0.113 eV for compositions in the system $La_{1-y}Sr_yCrO_3$ with $0.00 \leq y \leq 0.40$. Raffaelle *et al.* (*17*) reported activation energies of 0.182 and 0.194 eV for $LaCrO_3$ and $LaMnO_3$, respectively. In these studies it was concluded that conduction occurred by the small polaron mechanism. Thus, for $Y_{1-y}Ca_yMnO_3$, the calculated activation energies and the high linearity of the plots for $0.30 \leq y < 0.80$ in Fig. 1 are consistent with the assumption that electrical conduction in this compositional region occurs via the adiabatic small polaron mechanism.

The Seebeck coefficient is useful in analyzing electrical behavior, since it provides information about the concentration of charge carriers in a material. Heikes (*18*) derived the expression for small polaron conductors,

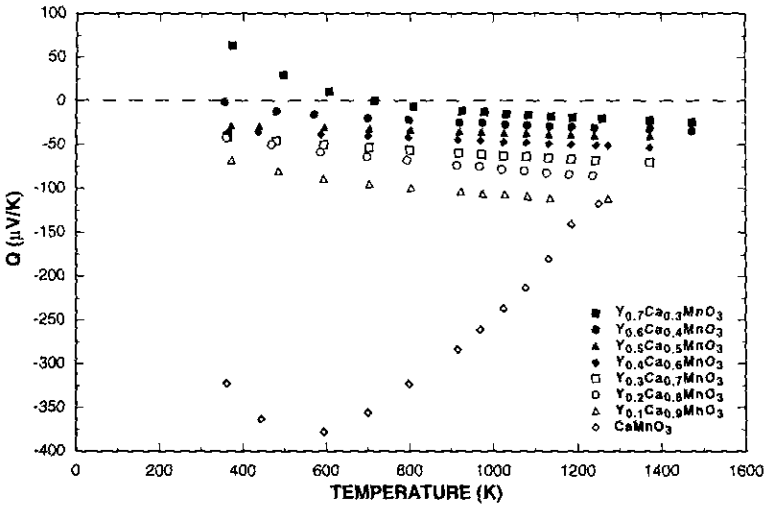

FIG. 2. Seebeck coefficient (Q) vs temperature in air for the indicated compositions.

$$Q = \pm \frac{k}{e}\left[\ln\left(\frac{1-C}{C}\right)\right] + S^{\circ}, \qquad (1)$$

where Q is the Seebeck coefficent, e is the absolute value of electron charge, C is the fraction of available hopping sites which are occupied, and S° is an entropy of transport term. A positive Q indicates that the carriers are holes, while Q is negative if the carriers are electrons. It will be noted that Eq. (1) does not allow for spin degeneracy of the carriers, implying that there is only one allowed spin orientation per site. Since neutron diffraction studies have indicated that ferromagnetic and antiferromagnetic coupling occurs in manganite perovskites (*19*), it is reasonable to assume that magnetic ordering fixes the spin orientation at each site. Since S° in oxides is generally small in magnitude (less than 10 μV/K (*20*)), it is frequently neglected, so that Eq. (1) rearranges to

$$C = 1\Big/\left[1 + \exp\left(\frac{Q}{86.17}\right)\right], \qquad (2)$$

where Q is in units of μ V/K.

Seebeck coefficients vs temperature for $Y_{1-y}Ca_yMnO_3$ ($0.30 \leq y \leq 1.00$) are shown in Fig. 2. While the Seebeck coefficient for $CaMnO_3$ showed considerable temperature dependence and had a relatively large magnitude at lower temperatures, Q for the other compositions was small in magnitude and exhibited only mild temperature dependence, except for $Y_{0.7}Ca_{0.3}MnO_3$ at low temperatures. The presence of the miscibility gap in the $Y_{1-y}Ca_yMnO_3$ system prevented the determination of the Seebeck coefficient across the entire system. Accordingly, Seebeck data was also obtained for the related system $La_{1-y}Ca_yMnO_3$ ($y = 0.00, 0.20, 0.40$, and 0.60) in which no miscibility gap occurs. Seebeck coefficients vs temperature for $La_{1-y}Ca_yMnO_3$ are shown in Fig. 3. For all compositions in Figs. 2 and 3, the Seebeck coefficient was negative at elevated temperatures.

The fraction of sites occupied, C, for $Y_{1-y}Ca_yMnO_3$ and $La_{1-y}Ca_yMnO_3$ were calculated from Eq. (2) using experimental Seebeck coefficients at 1273 K. The fraction of sites occupied is plotted vs composition in Fig. 4. The dashed line in the figure repre-

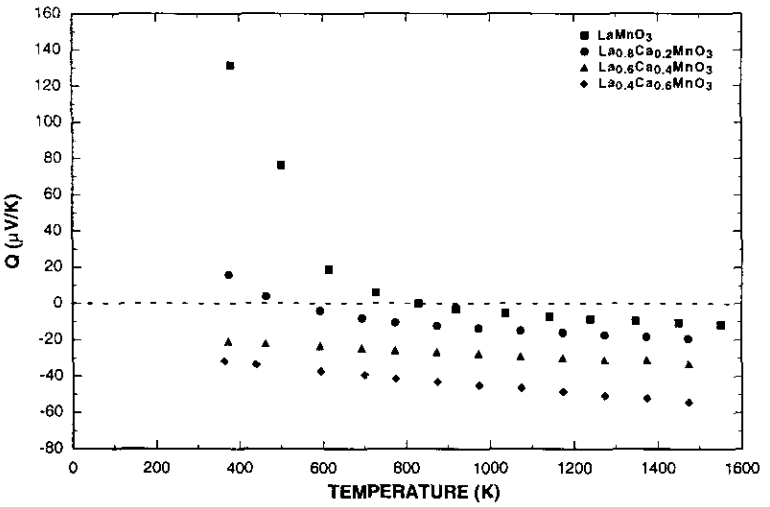

FIG. 3. Seebeck coefficient (Q) vs temperature in air for the indicated compositions.

sents the Seebeck behavior that would be expected in donor-doped $CaMnO_3$ if the oxygen stoichiometry was exactly 3.00 and Mn cations were present in the material only in the +3 and +4 valence states. According to the Verwey controlled-valency principle (*21*), substitution of Y^{3+} or La^{3+} ions for Ca^{2+} on the A sites will create charge carriers (electrons). Assuming these carriers are localized, each donor ion converts an Mn^{4+} to an Mn^{3+}. Thus, an increase in the Y^{3+} content would produce a linear increase in the concentration of Mn^{3+}, i.e., $[Y_{Ca}^{\cdot}] = [Mn_{Mn}^{\prime}]$ (using $CaMnO_3$ as the host lattice; [ ] refers to moles of the enclosed species per mole of oxide). The fraction of sites occupied, C, would steadily increase in magnitude (resulting in a decrease in the magnitude of Q) with increasing Y^{3+} content. At the midpoint of the system, $[Y_{Ca}^{\cdot}] = [Ca_{Ca}^{x}] = [Mn_{Mn}^{\prime}] = [Mn_{Mn}^{x}] = 0.50$. In this case, the conduction sites would be half-filled, so that $C = 0.50$ and $Q = 0.00$. As $[Y_{Ca}^{\cdot}]$ exceeded 0.50, $[Mn_{Mn}^{\prime}]$ would become greater than $[Mn_{Mn}^{x}]$, so that conduction would now be treated as occurring by the transport of electron holes associated with the Mn^{4+}. As the $[Y_{Ca}^{\cdot}]$ content approached 1.00, C should decrease toward 0.00 as $[Mn_{Mn}^{x}]$ decreased, resulting in an increase in magnitude of the (now positive) Seebeck coefficient. Thus, a negative Q corresponds to $[Mn^{4+}] > [Mn^{3+}]$, while a positive Q indicates $[Mn^{3+}] > [Mn^{4+}]$.

Figure 4 shows that the experimental results did not support this model. The composition with $y = 0.80$ was oxygen-deficient (the oxygen stoichiometry at 1273 K was determined thermogravimetrically to be 2.96). Assuming that the oxygen vacancies are doubly ionized, charge compensation may occur by the conversion of two Mn ions from the +4 to the +3 valence state. The Y^{3+} content and this oxygen deficiency account for the observed higher than predicted C value. For $y = 0.70$, C was essentially equivalent to the value predicted by the above model. However, for $y < 0.70$, while C continued to increase with increasing Y^{3+} content, it failed to reach 0.50 for $y = 0.50$. Even when y was as low as 0.30, Q remained negative (although very small in magnitude). It should be noted that the model above assumed that donors or acceptors were

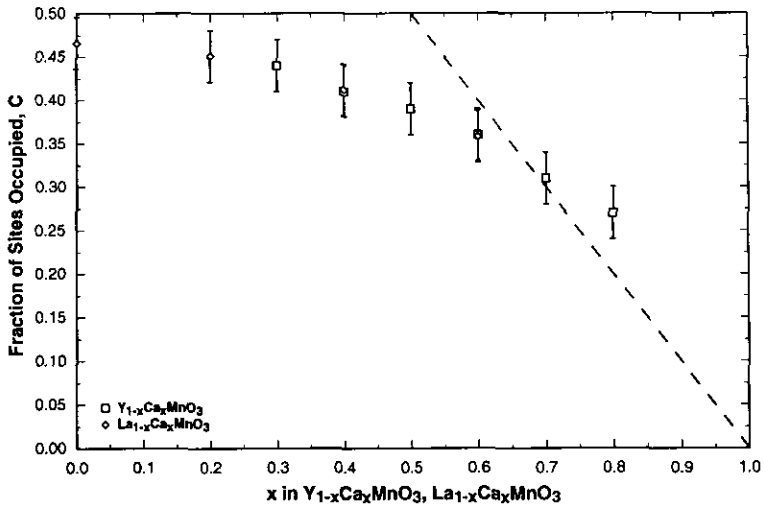

FIG. 4. Fraction of sites occupied (C) vs Ca content in air at 1273 K.

compensated electronically. Since the data did not follow that model, it was important to consider the possibility of ionic compensation. However, in the compositional region in which the negative deviation from the classic model was observed, the materials were either stoichiometric or very nearly so (as determined by thermogravimetric analysis and/or iodometric titration). The absence of an excess concentration of either cation or anion vacancies indicates that, in these materials, the cation and anion vacancies were present in essentially stoichiometric quantities so that they charge compensated each other. It was therefore concluded that those ions which carry a charge with respect to the host lattice were compensated electronically. The fact that the observed Seebeck behavior for $y < 0.70$ could not be explained under the assmption that only trivalent and tetravalent Mn ions were present led to consideration of the possibility that other valence states of Mn occur in these materials.

Previous studies (*17, 22*) have indicated that Mn^{3+} in crystalline solids is subject to a thermally activated disproportionation,

$$2\,Mn^{3+} \rightleftarrows Mn^{4+} + Mn^{2+} \qquad (3)$$

with the associated equilibrium constant, K_D,

$$K_D = \frac{[Mn^{4+}][Mn^{2+}]}{[Mn^{3+}]^2} = \exp\left[\frac{-\Delta G_D^\circ}{kT}\right], \qquad (4)$$

where ΔG_D° is the free energy of disproportionation.

It was assumed that when divalent Mn ions are present they do not participate in the conduction process, i.e., electrical conduction within the crystal occurs only by hopping of electrons from Mn^{3+} to adjacent Mn^{4+} cations. The Mn^{2+} cations therefore act as site-blockers for conduction. Support for this assumption was found in the results of a study by Yu *et al.* (*23*) which determined that in $LaCrO_3$ the mobility of carriers associated with Cr^{2+} ions was lower by at least an order of magnitude than the mobility of carriers hopping between Cr^{3+} and Cr^{4+} ions. Similarly, Dorris and Mason (*22*) concluded that Mn_3O_4 contained divalent Mn^{2+} due to disproportionation but conduction occurred solely via the hopping of carriers between Mn^{3+} and Mn^{4+} ions.

Since Q was negative for these compositions, the carriers were considered to be electrons associated with the Mn^{3+}. Using $YMnO_3$ as the host lattice ($[Mn_{Mn}^{\cdot}] = [Mn^{4+}]$, $[Mn_{Mn}^{x}] = [Mn^{3+}]$, and $[Mn_{Mn}^{\prime}] = [Mn^{2+}]$), the fraction of available sites occupied can be written as

$$C = \frac{[Mn_{Mn}^{x}]}{[Mn_{Mn}^{x}] + [Mn_{Mn}^{\cdot}]}. \quad (5)$$

The mass balance equation for Mn is

$$[Mn_{Mn}^{\prime}] + [Mn_{Mn}^{x}] + [Mn_{Mn}^{\cdot}] = 1.00. \quad (6)$$

The electroneutrality condition for the crystal is

$$3[V_M^{\prime\prime\prime}] + [Mn_{Mn}^{\prime}] + [Ca_Y^{\prime}] = [Mn_{Mn}^{\cdot}] + 2[V_O^{\cdot\cdot}] \quad (7)$$

where $[V_M^{\prime\prime\prime}]$ refers to both A-site and B-site vacancies.

This system of three equations was solved to obtain the concentrations of the three valence states of Mn at 1273 K. The site occupancy, C, was obtained from the Seebeck data and the amount of oxygen or cation deficiency was determined by thermogravimetric analysis and/or iodometric titration. (For $LaMnO_3$, the oxygen stoichiometry reported by Kuo *et al.* (*3*) was used).

Solution of the system of equations for each composition yielded the following formulae:

$La(V_{La}^{\prime\prime\prime})_{0.03}Mn_{0.23}^{\prime}Mn_{0.36}^{x}Mn_{0.41}^{\cdot}(V_{Mn}^{\prime\prime\prime})_{0.03}O_{3.09}$
$La_{0.800}Ca_{0.200}^{\prime}(V_{La}^{\prime\prime\prime})_{0.007}Mn_{0.200}^{\prime}Mn_{0.358}^{x}Mn_{0.442}^{\cdot}(V_{Mn}^{\prime\prime\prime})_{0.007}O_{3.020}$
$La_{0.60}Ca_{0.40}^{\prime}Mn_{0.12}^{\prime}Mn_{0.36}^{x}Mn_{0.52}^{\cdot}O_{3.00}$
$Y_{0.70}Ca_{0.30}^{\prime}Mn_{0.17}^{\prime}Mn_{0.36}^{x}Mn_{0.47}^{\cdot}O_{3.00}$
$Y_{0.60}Ca_{0.40}^{\prime}Mn_{0.12}^{\prime}Mn_{0.36}^{x}Mn_{0.52}^{\cdot}O_{3.00}$
$Y_{0.50}Ca_{0.50}^{\prime}Mn_{0.07}^{\prime}Mn_{0.36}^{x}Mn_{0.57}^{\cdot}O_{3.00}$
$Y_{0.40}Ca_{0.60}^{\prime}Mn_{0.03}^{\prime}Mn_{0.36}^{x}Mn_{0.61}^{\cdot}O_{2.99}(V_O^{\cdot\cdot})_{0.01}$
$Y_{0.30}Ca_{0.70}^{\prime}Mn_{0.01}^{\prime}Mn_{0.32}^{x}Mn_{0.67}^{\cdot}O_{2.98}(V_O^{\cdot\cdot})_{0.02}$.

These formulae are consistent with the observed negative values of Q for these compositions since, under the assumption that conduction is essentially confined to the Mn^{3+} and Mn^{4+} sites, $[Mn^{4+}]$ exceeds $[Mn^{3+}]$ in each case.

Considering the compositions in both systems as a whole, it appears that as the Ca^{2+} content increases from 0.00 to 1.00, charge compensation is initially achieved through an increase in the Mn^{4+} concentration at the expense of Mn^{2+}, leaving the Mn^{3+} concentration essentially unchanged. Only as the divalent Mn is eliminated (at high Ca contents) does compensation occur via conversion of the Mn^{3+} to Mn^{4+}. If no oxygen deficiency occurred at the high Ca^{2+} end, only Mn^{4+} would be present in the $CaMnO_3$ end member. Since oxygen deficiency does occur (the room temperature oxygen stoichiometry was determined iodometrically to be 2.94), a substantial Mn^{3+} content appears even in $CaMnO_3$.

The calculated concentrations of the three valence states of Mn in the compositions under study allowed values of the equilibrium constant K_D to be estimated from Eq. (4), assuming that the activity of each species was equivalent to its concentration. The resulting values of K_D are listed in Table I. The high degree of uncertainty in the values results from the uncertainty of ± 0.02 in the calculated concentrations of the three va-

lence states of Mn. These values for K_D are much higher than those obtained by Kuo (*14*) for compositions in the system $La_{1-y}Sr_yMnO_3$ (also listed in Table I) using a different defect model.

The Seebeck coefficient for $LaMnO_3$ showed considerable temperature dependence at lower temperatures. As the temperature decreased, the negative Q decreased to zero and then became positive in sign with steadily increasing magnitude. This behavior is consistent with the disproportionation model. Since the disproportionation is thermally excited, as the temperature decreased the amount of disproportionation in the crystal would be expected to decrease, resulting in a reduction in $[Mn'_{Mn}]$ and $[Mn^{\cdot}_{Mn}]$ and an increase in $[Mn^{x}_{Mn}]$. Application of Eqs. (5), (6), and (7) at 825 K yielded the following formula:

$$La(V'''_{La})_{0.03}Mn'_{0.22}Mn^{x}_{0.39}Mn^{\cdot}_{0.39}(V'''_{Mn})_{0.03}O_{3.09}.$$

For purposes of calculation, the oxygen stoichiometry was assumed to remain constant at 3.09, since no data regarding the oxygen stoichiometry of $LaMnO_3$ at lower temperatures was available. As expected, $[Mn'_{Mn}]$ and $[Mn^{\cdot}_{Mn}]$ decreased and $[Mn^{x}_{Mn}]$ increased. At 500 and 380 K (again assuming that the oxygen stoichiometry was unchanged) the calculated formulae were:

$$La(V'''_{La})_{0.03}Mn'_{0.08}Mn^{x}_{0.66}Mn^{\cdot}_{0.26}(V'''_{Mn})_{0.03}O_{3.09}$$

and

$$La(V'''_{La})_{0.03}Mn^{x}_{0.82}Mn^{\cdot}_{0.18}(V'''_{Mn})_{0.03}O_{3.09}.$$

The positive sign for Q is consistent with the fact that at these temperatures, $[Mn^{4+}] < [Mn^{3+}]$. At 380 K, the disproportionation has apparently been entirely suppressed as only trivalent and tetravalent Mn remain.

TABLE I

CALCULATED VALUES OF K_D FOR THE INDICATED COMPOSITIONS AT 1273 K

Composition	K_D
$Y_{0.7}Ca_{0.3}MnO_3$	0.62 ± 0.19
$Y_{0.6}Ca_{0.4}MnO_3$	0.48 ± 0.17
$Y_{0.5}Ca_{0.5}MnO_3$	0.31 ± 0.15
$Y_{0.4}Ca_{0.6}MnO_3$	0.14 ± 0.13
$Y_{0.3}Ca_{0.7}MnO_3$	$0.07^{+0.15}_{-0.07}$
$LaMnO_3$	0.73 ± 0.20
$La_{0.8}Ca_{0.2}MnO_3$	0.69 ± 0.20
$La_{0.6}Ca_{0.4}MnO_3$	0.48 ± 0.17
$LaMnO_3$[a]	0.010
$La_{0.95}Sr_{0.05}MnO_3$[a]	0.007
$La_{0.9}Sr_{0.1}MnO_3$[a]	0.093
$La_{0.8}Sr_{0.2}MnO_3$[a]	0.132

[a] Reference (*14*).

TABLE II

TEMPERATURE DEPENDENCE OF K_D AND ΔG°_D FOR $LaMnO_3$ IN AIR

Temperature (K)	K_D	ΔG°_D (eV)
1273	0.73 ± 0.20	0.035 ± 0.030
825	0.56 ± 0.15	0.041 ± 0.022
500	0.05 ± 0.02	0.129 ± 0.022

Equation (4) was used to obtain values of K_D for $LaMnO_3$ as a function of temperature. The calculated values are listed in Table II. As expected, K_D approached a value of 1.00 with increasing temperature. Values of the free energy of disproportionation, ΔG°_D, were calculated using the relation

$$\Delta G^\circ_D = -kT \ln K_D, \tag{8}$$

where k is Boltzmann's constant and T is absolute temperature. The resulting values are also listed in Table II. The enthalpy of disproportionation, ΔH°_D, for $LaMnO_3$ (calculated from the van't Hoff equation) was 0.20 ± 0.05 eV. The upper limit of this value (0.25 eV) is close to the value of 0.27 eV reported for ΔH°_D in Mn_3O_4 (*22*).

Carrier drift mobility, μ, can be written as

$$\mu = \frac{\sigma}{(NC)e}, \tag{9}$$

where σ is electrical conductivity and N is the density of available sites. There are four formula units per cell, so the concentration of Mn is $4/V_c$, where V_c is the volume of the cell. Since only the trivalent and tetravalent Mn ions are believed to participate in the conduction process, the density of available sites, N, is

$$N = \left[\frac{4}{V_c}\right]([Mn^x_{Mn}] + [Mn^{\cdot}_{Mn}]). \quad (10)$$

The combination of Eqs. (5) and (10) yields

$$NC = \left[\frac{4}{V_c}\right]([Mn^x_{Mn}]). \quad (11)$$

Therefore,

$$\mu = \frac{\sigma V_c}{4e[Mn^x_{Mn}]}. \quad (12)$$

The calculated mobilities at 1273 K are listed in Table III. These mobilities are somewhat higher than the mobilities reported for compositions in $La_{1-y}Sr_yMnO_3$ (*1*). In that system, the mobilities at 1273 K ranged from approximately 0.040 to approximately 0.065 cm^2/V-sec for $0.00 \leq y \leq 0.20$. The calculated mobilities are also higher than those reported for the system $Y_{1-y}Ca_yCrO_3$, in which mobilities were between 0.03 and 0.05 cm^2/V-sec for $0.00 \leq y \leq 0.20$ (*5*).

TABLE III

CALCULATED DRIFT MOBILITIES FOR THE INDICATED COMPOSITIONS IN AIR

Composition	μ (cm^2/V-sec) at 1273 K	μ (cm^2/V-sec) at 298 K
$Y_{0.7}Ca_{0.3}MnO_3$	0.11	1.1×10^{-3}
$Y_{0.6}Ca_{0.4}MnO_3$	0.14	2.2×10^{-3}
$Y_{0.5}Ca_{0.5}MnO_3$	0.15	0.01
$Y_{0.4}Ca_{0.6}MnO_3$	0.20	0.03
$Y_{0.3}Ca_{0.7}MnO_3$	0.21	0.08
$Y_{0.2}Ca_{0.8}MnO_3$	0.20	0.24
$La_{0.8}Ca_{0.2}MnO_3$	0.16	6.8×10^{-3}
$La_{0.6}Ca_{0.4}MnO_3$	0.22	0.07

The calculated room temperature mobilities are also listed in Table III. The fact that the room temperature mobility for $y = 0.80$ is greater than the mobility as 1273 K supports the previously stated assumption that the small polaron mechanism is not applicable to the highest Ca compositions in $Y_{1-y}Ca_yMnO_3$.

4. Conclusion

Compositions in the system $Y_{1-y}Ca_yMnO_3$ are single-phase solid solutions for $y \geq 0.30$. The electrical conduction for compositions with $0.30 \leq y < 0.80$ appears to be due to a small polaron mechanism. The assumption that the Mn ions are present only in the +3 and +4 valence states was inconsistent with the observed Seebeck behavior. A defect model was developed which incorporated the thermally excited disproportionation of Mn^{3+} into Mn^{2+} and Mn^{4+}. The observed Seebeck data were then explained by assuming that Mn^{2+} acts as a site-blocker. Simultaneous solution of the equations for fraction of sites occupied, mass balance, and electroneutrality allowed the concentrations of the three valence states of Mn to be calculated for a given composition at a given temperature.

Acknowledgments

This research was supported by the Basic Energy Science Division and Morgantown Energy Technology Center of the United States Department of Energy.

References

1. J. H. KUO, H. U. ANDERSON, AND D. M. SPARLIN, *J. Solid State Chem.* **87,** 55 (1990).
2. S. SRILOMSAK, D. P. SCHILLING, AND H. U. ANDERSON, *in* "Proc. 1st Intl. Symp. on Solid Oxide Fuel Cells" (S. C. Singhal, Ed.), Electrochem. Soc. Proc., Vol. 89-11, p. 214 (1989).
3. J. H. KUO, H. U. ANDERSON, AND D. M. SPARLIN, *J. Solid State Chem.* **83,** 52 (1989).
4. D. P. KARIM AND A. T. ALDRED, *Phys. Rev. B* **20,** 2255 (1979).
5. G. F. CARINI II, H. U. ANDERSON, D. M. SPAR-

LIN, AND M. M. NASRALLAH, *Solid State Ionics,* in press.
6. W. J. WEBER, C. W. GRIFFIN, AND J. L. BATES, *J. Am. Ceram. Soc.* **70,** 265 (1987).
7. O. YAMAMOTO, Y. TAKEDA, R. KANNO, AND M. NODA, *Solid State Ionics* **22,** 241 (1987).
8. A. MACKOR, C. SPEE, E. VAN DER ZOUWEN-ASSINK, J. BAPTISTA, AND J. SCHOONMAN, *in* "Proc. Intersoc. Energy Convers. Eng. Conf., 25th," Vol. 3, p. 251 (1990).
9. M. P. PECHINI, U.S. PATENT 3,330,697 (1967).
10. V. WOOD, A. AUSTIN, E. COLLINGS, AND K. BROG, *J. Phys. Chem. Solids* **34,** 859 (1973).
11. H. L. YAKEL, W. C. KOEHLER, E. F. BERTAUT, AND E. F. FORRAT, *Acta Crystallogr.* **16,** 957 (1963).
12. R. D. SHANNON, *Acta Crystallogr. Sect. A* **32,** 751 (1976).
13. E. POLLERT, S. KRUPICKA, AND E. KUZMICOVA, *J. Phys. Chem. Solids* **43,** 1137 (1982).
14. J. H. KUO, "Studies of Defect Structure and Oxidation-Reduction Behavior of Undoped $LaMnO_3$, Sr-Doped $LaMnO_3$, and Mg-Doped $LaMnO_3$," Ph.D. Dissertation, University of Missouri–Rolla (1987).
15. G. H. JONKER, Physica **20,** 1118 (1954).
16. G. V. SUBBA RAO, B. M. WANKLYN, AND C. N. R. RAO, *J. Phys. Chem. Solids* **32,** 345 (1971).
17. R. RAFFAELLE, H. U. ANDERSON, D. M. SPARLIN, AND P. E. PARRIS, *Phys. Rev. B.* **43,** 7991 (1991).
18. R. R. HEIKES, *in* "Thermoelectricity: Science and Engineering" (R. R. Heikes and R. W. Ure, Jr., Eds.), Interscience, New York (1961).
19. E. O. WOLLAN AND W. C. KOEHLER, *Phys. Rev.* **100,** 545, (1955).
20. J. B. GOODENOUGH, *Mater. Res. Bull.* **5,** 621 (1970).
21. E. J. W. VERWEY, P. W. HAAIJMAN, J. C. ROMEIJN, AND G. W. VAN OOSTERHOUT, *Philips Res. Rep.* **5,** 173 (1950).
22. S. E. DORRIS AND T. O. MASON, *J. Am. Ceram. Soc.* **71,** 379 (1988).
23. C. J. YU, H. U. ANDERSON, AND D. M. SPARLIN, *J. Solid State Chem.* **78,** 242 (1989).